AMS Copyright Notice

Convective Episodes in the East-Central United States

MATTHEW D. PARKER

Department of Marine, Earth, and Atmospheric Sciences, North Carolina State University, Raleigh, North Carolina

DAVID A. AHIJEVYCH

National Center for Atmospheric Research, Boulder, Colorado

(Manuscript received 20 November 2006, in final form 20 February 2007)

ABSTRACT

Nine years of composited radar data are investigated to assess the presence of organized convective episodes in the east-central United States. In the eastern United States, the afternoon maximum in thunderstorms is ubiquitous over land. However, after removing this principal diurnal peak from the radar data, the presence and motion of organized convective systems becomes apparent in both temporally averaged fields and in the statistics of convective episodes identified by an objective algorithm. Convective echoes are diurnally maximized over the Appalachian chain, and are repeatedly observed to move toward the east. Partly as a result of this, the daily maximum in storms is delayed over the Piedmont and coastal plain relative to the Appalachian Mountains and the Atlantic coast. During the 9 yr studied, the objective algorithm identified 2128 total convective episodes (236 yr^{-1}), with several recurring behaviors. Many systems developed over the elevated terrain during the afternoon and moved eastward, often to the coastline and even offshore. In addition, numerous systems formed to the west of the Appalachian Mountains and moved into and across the eastern U.S. study domain. In particular, many nocturnal convective systems from the central United States entered the western side of the study domain, frequently arriving at the eastern mountains around the next day's afternoon maximum in storm frequency. A fraction of such well-timed systems succeeded in crossing the Appalachians and continuing across the Piedmont and coastal plain. Convective episodes were most frequent during the high-instability, low-shear months of summer, which dominate the year-round statistics. Even so, an important result is that the episodes still occurred almost exclusively in above-average vertical wind shear. Despite the overall dominance of the diurnal cycle, the data show that adequate shear in the region frequently leads to long-lived convective episodes with mesoscale organization.

1. Introduction

At least since the work of Wallace (1975), it has been well established that thunderstorms have an afternoon maximum across most of the conterminous United States. This diurnal maximum is particularly strong over the eastern and southeastern United States, but is actually overwhelmed by the signal of nocturnal convective storms in the Great Plains. Frequent, long-lived mesoscale convective systems (MCSs) that cross the central United States are now known to explain this nocturnal maximum.

Pioneering work by Maddox (1980), Cotton et al. (1983), and others revealed the predominant role of the Rocky Mountains in this nocturnal maximum. These and other studies have found that precursor storms for nocturnal MCSs often develop along the eastern slopes of the Rockies. The storms are then sustained by a nocturnal low-level jet over the plains (Trier and Parsons 1993; Augustine and Caracena 1994), which many investigators have linked to the sloped terrain over the west-central United States (e.g., Bonner and Paegle 1970; McNider and Pielke 1981). Studies such as those by Tripoli and Cotton (1989), Grady and Verlinde (1997), and Tucker and Crook (1999) have highlighted

Corresponding author address: Dr. Matthew Parker, North Carolina State University, Campus Box 8208, Raleigh, NC 27695-8208.
E-mail: mdparker@ncsu.edu

DOI: 10.1175/2007MWR2098.1

the merging and downslope spreading of outflows from afternoon mountain thunderstorms in the genesis of MCSs. This outflow must sometimes pass through a zone of suppression under the subsiding branch of the solenoidal circulation that is produced by heating of the high terrain (Tripoli and Cotton 1989), but, thereafter, the convection is reinvigorated by unstable air lying farther to the east.

The east-central United States is not generally thought to be as favorable as the plains for recurring nocturnal MCSs, although low-level jets (Bonner 1968; Zhang et al. 2006) and elevated mixed layers (e.g., Farrell and Carlson 1989) are occasionally observed in the lee of the Appalachians. Despite the relative scarcity of these ingredients, the agglomeration of outflows from mountain convection over the Appalachians, when paired with the frequent presence of moist unstable air over the southeastern United States, suggests a mechanism for upscale growth similar to that reviewed by Tucker and Crook (1999).

Carbone et al. (2002) noted that diurnal forcing for convection predominates over the Rockies, but that a semidiurnal mode with a nocturnal maximum appears over the Great Plains in association with eastward-moving envelopes of mesoscale convective precipitation. This nocturnal maximum over the central United States was tied to a corridor of eastward-moving precipitation systems that had their origins over the Rocky Mountains and high plains. In contrast, the predominant eastern U.S. signal in their data was a strong afternoon maximum in radar echoes over the Ohio and Tennessee Valleys and the eastern mountains (their Fig. 12). However, their study domain did not extend much past the Appalachian chain; understandably, much of their focus was on the diurnal–nocturnal cycle of large, intense convective systems that repeatedly traverse the Great Plains.

Our original interest in the problem of convective systems over the eastern United States was piqued by the east's gross similarities in geography to the west-central United States. In the Virginias and North Carolina, the Blue Ridge Mountains rise roughly 1 km above the eastern coastal plain (Fig. 1). Convective storms develop over the Appalachian chain during the afternoon, and can then propagate downslope toward the east where boundary layer moisture is plentiful. In lieu of a nocturnal low-level jet, if eastward-moving convective systems survive long enough, they could be sustained by the comparatively warm coastal waters of the Atlantic by nightfall, with the Gulf Stream only slightly farther offshore.

A climatology of severe thunderstorm winds (Doswell et al. 2005) reveals a maximum in frequency extending from north-central Georgia through central North Carolina, which begins in May, peaks in July, and persists through August. In part, this corresponds with the corridor for "stationary frontal" derechos, which curves around the southern end of the Appalachians as diagnosed by Evans and Doswell (2001). But it is also interesting to note that the location of the summertime apex in severe wind reports (Doswell et al. 2005, their Fig. 13d) is just downstream of the tallest part of the Blue Ridge Mountains (from roughly 34.5° to 37°N in Fig. 1). This suggests a possible relationship to the terrain, and an obvious hypothesis is that the elevated heat island effect of the mountains is a favorable location for convective initiation. CAPE is frequently present over the lower-lying areas of the Piedmont and the coastal plain, such that the orogenic storms would often move into an unstable environment and become severe.

Interestingly, the diurnal Hovmöller diagrams of Carbone et al. (2002) also showed that the signal of eastward-moving nocturnal convective systems over the central United States would arrive at the Appalachians during the late afternoon of the following day. This phasing may lead to the reintensification of convection as the envelope of a precursor precipitation system approaches the eastern mountains. In some cases, such systems might even be able to cross the Appalachian chain and survive on the eastern side.

Evans and Doswell (2001, their Fig. 3) found that a majority of the derechos they studied ended on the western periphery of the Appalachian Mountains, but documented a few cases that survived while traversing them. In fact, their climatological corridor for "hybrid" derechos passes over the tallest part of the Blue Ridge, from Kentucky and Tennessee into Virginia and North Carolina. Because Appalachian-crossing convective systems are a concern for operational forecasts in the eastern Piedmont, recent studies have begun to investigate the dynamics governing convective systems' interactions with mountainous terrain. Frame and Markowski (2006) reviewed the scant literature on the topic and addressed the roles of peak height and spacing upon a mountain-crossing convective system; we recount their results in more detail during the course of our discussion in section 4.

Certainly, there are some MCSs in the central United States that do not begin over the Rockies, and the same result must be expected for organized convection east of the Appalachians. In addition to convective initiation along synoptic fronts, Koch and Ray (1997) noted that storms are often initiated along Piedmont troughs east of the mountains in North Carolina, as well as along sea-breeze fronts on the Atlantic coast. Given this variety of initiation mechanisms, as well as the first-

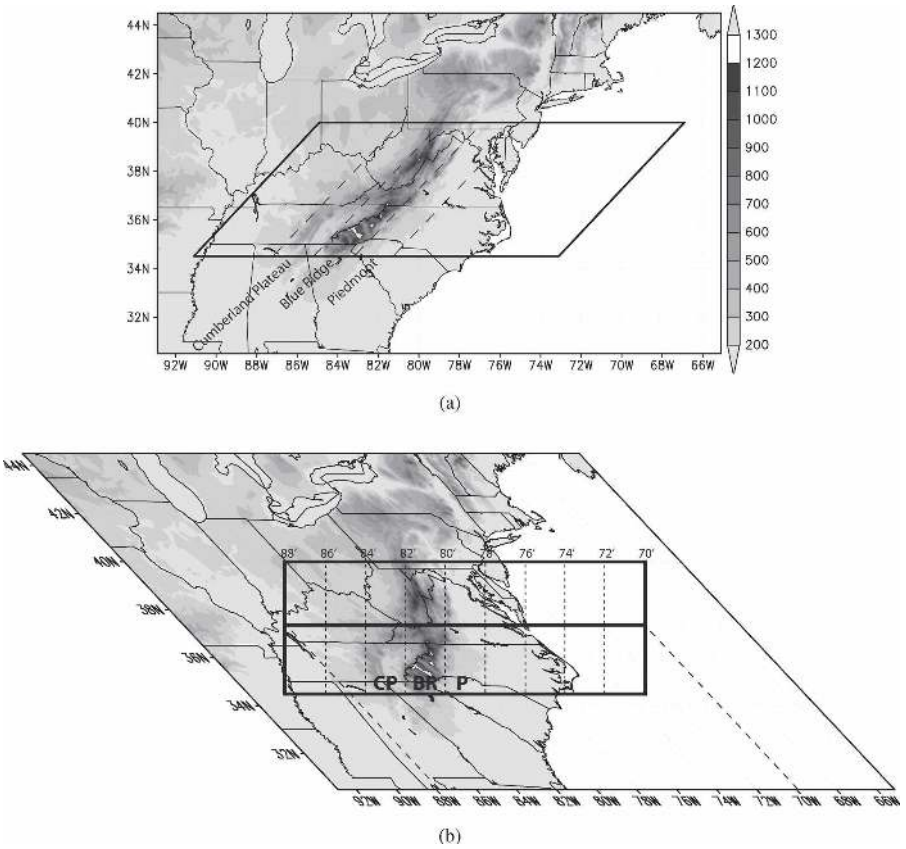

FIG. 1. Surface elevation (m) in the region of this study (land only). (a) Mercator projection, with the window for the longitude-shifted Hovmöller diagrams (Fig. 3, etc.) outlined by a parallelogram. (b) Skewed projection using the linear translation of longitude described in the text. The window for the longitude-shifted Hovmöller diagrams (Fig. 3, etc.) is outlined by a rectangle, with the "corrected" longitudes (lon_{new}) labeled above. Topographic features of interest are also labeled [names in (a), abbreviations in (b)].

order similarities in terrain between the Front Range of the Rockies and the Blue Ridge front in Appalachia, we hypothesized that long-lived convective systems are common to the east-central United States. Indeed, removing the diurnal afternoon maximum in storms from our data reveals their signatures.

This study uses 9 yr's worth of radar data in order to quantify the frequency and behavior of coherent convective *episodes*[1] in the eastern United States. In section 2 we review the radar dataset we used and our methods of analysis. We then present our results in terms of the averaged spatial and temporal structures in the dataset (section 3) and in terms of the properties of individual, objectively identified convective episodes (section 4). We also consider whether the peak summer months are consistent with the full-year data (section 5). The paper then concludes with a summary and some suggested avenues for future work.

2. Data and methods

Our analyses incorporate the Weather Systems International (WSI) Corporation's NOWrad national composites, or summaries, of Weather Surveillance Radar-1988 Doppler (WSR-88D) reflectivity data for 9 yr: 1996–2000 and 2002–05. We omitted 2001 because the data were missing for 1 January to 3 May. We performed our analyses for full years in order to be exhaustive, as convection can occur during any month in the southeastern United States. To assess the contributions of the warm season storms to our totals, we also computed our statistics for June–August separately (see section 5).

[1] Carbone et al. (2002) defined an episode as a space–time cluster of heavy precipitation resulting from sequences of organized convection such as mesoscale convective systems. In this paper, "episode" refers to such a signal as detected using the methods in section 2.

To create the NOWrad composites, raw data on a polar grid of 1° × 1 km from each radar are converted to a Cartesian grid with nominal temporal, spatial, and reflectivity intervals of 15 min, 2 km × 2 km, and 5 dBZ. Each pixel's value is the largest reflectivity measured in a 15-min interval by any radar in a column above a point, with the exception that reflectivity from radars within 230 km of a point[2] is given priority over reflectivity from radars beyond 230 km. Near the center of the raw polar grid, where oversampling occurs during conversion to the Cartesian grid, the largest reflectivity is used. When a cone of silence above a radar is not filled by reflectivity from another radar within 230 km, extended-range reflectivity from the nearest radars is used. Automated computer algorithms at WSI filter bad data from individual WSR-88Ds and from the national composite before a radar meteorologist removes by hand most remaining artifacts, including anomalous propagation echoes. NOWrad data cover most of the conterminous United States.

Following Parker and Knievel (2005), we call each echo that is ≥40 dBZ a *storm element* (or, more briefly, a *storm*). Other researchers have used the same or similar thresholds to diagnose thunderstorms and to discriminate between convective and stratiform rain (e.g., Gamache and Houze 1982; Falconer 1984; Rickenbach and Rutledge 1998). Parker and Knievel (2005) noted some of the shortcomings of this approach and of the NOWrad dataset in general, including biases introduced by nonconvective echoes above 40 dBZ, coverage and range dependencies, beam blocking, and differing calibration among radar sites. Without rehashing their discussion, in the present paper we discuss possible systematic impacts of these effects as they arise in the text. In particular, we address the possible role of >40 dBZ cold season bright bands by analyzing only the months of June–August in section 5. Notwithstanding the dataset's caveats, the method remains useful because the data have excellent coverage in space and time, while the 40-dBZ threshold makes for a compact representation of convective signals in the large dataset.

For our calculations, we defined the binary "storm" variable i_{40},

$$i_{40}(x, y, t) = \begin{cases} 1 \\ 0 \end{cases} \quad \text{when} \quad \begin{matrix} \text{dB}Z(x, y, t) \geq 40 \\ \text{dB}Z(x, y, t) < 40 \end{matrix}, \qquad (1)$$

and then computed the following statistic at each point for the n days in the 9-yr sample:

[2] For reference, the nominal base scan radar beam height is approximately 5 km AGL at the 230-km range.

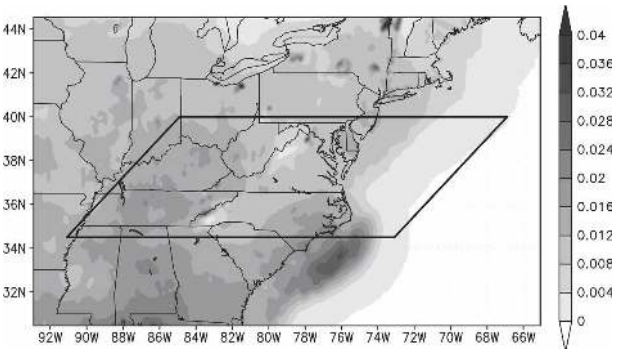

FIG. 2. Fractional storm frequency, Pr_{storm}, over the region of this study. The maximal shading level corresponds to "storms" occurring at a point more than 4% of the time during the 9-yr period. The window for the longitude-shifted Hovmöller diagrams (Fig. 3, etc.) is outlined by a parallelogram.

$$\text{Pr}_{\text{storm}}(x, y, t) = \frac{1}{n} \sum_{t=1}^{n} i_{40}(x, y, t). \qquad (2)$$

Here, Pr_{storm} is the probability, or frequency (Wilks 1995), that the point (x, y) had a storm at time-of-day t on a randomly selected day (e.g., Fig. 2).

Notably, we compared the results from this method to results that we obtained using the method of Carbone et al. (2002), in which the NOWrad reflectivities were converted to estimated rainfall rates. The results were very similar (the correlation of the two datasets is 0.97), and we chose the Pr_{storm} method because it more clearly depicted the contributions from convective storms, while avoiding some of the ambiguities[3] involved in a one-size-fits-all $Z - R$ relationship. As well, the Pr_{storm} approach enabled us more directly to compare our results to those of Ahijevych et al. (2004, e.g., their Figs. 1, 3, and 8) as well as Parker and Knievel (2005).

To expedite the analysis and reduce the array size for our calculations, the original reflectivity data were remapped to a 10 km × 10 km grid using the maximal reflectivity in each 10 km × 10 km grid box; in other words, if a pixel exceeded 40 dBZ anywhere within the 10 km × 10 km box, then i_{40} was 1 for that box. We were interested in convective systems throughout the region, but we also focused particularly on the latitudes at which the Appalachian Mountain chain is the tallest. The window from 34.5° to 40°N encompasses most of

[3] We did not want to overemphasize the heavy precipitation of isolated strong storms, since they are relatively infrequent. And, because we were using data from both the cold and warm seasons, we did not want to identify synoptic cyclones with widespread moderate rainfall in our analyses.

the terrain above 750 m MSL in the mid-Atlantic states. Presumably, whatever impact the Appalachians may have on precipitation systems will be maximized in this region. This window is also of interest because the Appalachians are farther from the coast here than in the Northeast, providing for a larger area of radar coverage downstream of the terrain.

Because we specifically sought the possible impacts of the Appalachian Mountain chain and the eastern coastline upon precipitation systems, we performed a translation of the longitudes following the method of Ahijevych et al. (2004). The rearranged coordinates (based on the center latitude of the north–south window) were given by

$$\text{lon}_{\text{new}} = \text{lon}_{\text{old}} + (\text{lat} - 37.25^\circ)\frac{10}{9}. \qquad (3)$$

The effect of this transformation is to straighten the Appalachian chain, and to make the coastline more nearly meridional in the area of emphasis (the quadrilaterals in Fig. 1).

Our linear translation of longitudes implicitly assumes that convective systems move predominantly in the zonal direction. However, we also considered the possibility that the systems' motions were predominantly perpendicular to the mountains and the coastline. We tried reorienting the study region 52° clockwise, producing a domain that extended southeastward from the highest part of the Appalachian Mountains, crossing the coastline from Cape Hatteras through Georgia (not shown). While this was appealing because the coastline to the southeast is almost parallel to the Appalachians, ultimately this approach simply muddled the radar-derived statistics and made the systems' signals more difficult to detect. More detailed analyses and radar animations revealed that most of the regional precipitation systems move eastward rather than southeastward (i.e., perpendicular to the terrain). Therefore, only results from the longitudinal translation are reported upon here.

We sought to understand whether long-lived convective systems frequent the eastern United States. To quantify the behavior of convection within the study domain depicted in Fig. 1, we used two complementary approaches. The first was an analysis of the temporally and spatially averaged structures from the entire 9-yr dataset. To look at the recurring convective signals that were present, we analyzed the dataset's principal components of variability, that is, its empirical orthogonal functions (EOFs; Lorenz 1956).

We did not consider our initial temporal–spatial analyses sufficient for rejecting the hypothesis that there is an eastward-moving MCS signal in the eastern United States, nor for rejecting the null hypothesis. Some patterns compatible with moving mesoscale convective systems appeared. However, because the dataset includes many different kinds of convective storms and patterns over the 9-yr period, these appearances may be deceiving. Convection may simply develop at different longitudes at different times, which could account for the observed patterns without individual convective storms having moved. For this reason, it was necessary to identify individual convective episodes and to catalog their recurring behaviors.

Therefore, our second approach was an "object oriented" technique in which individual convective episodes were identified by an algorithm similar to that used by Carbone et al. (2002) and Ahijevych et al. (2004). Because moving convective episodes appear as swaths of $\text{Pr}_{\text{storm}} > 0$ within Hovmöller diagrams, such episodes can be identified objectively and automatically by comparing a streaklike function to the Hovmöller data. A streak-fitting function was devised to mirror the properties of the observed streaks in the Hovmöller data: the function was constant in the along-streak direction, with a length equivalent to 2° longitude,[4] and was a cosine function in the across-streak direction, with a width equivalent to 3 h. For each time and longitude, this streak-fitting function was rotated through the range of angles representing speeds from -20 through 35 m s^{-1} in the Hovmöller diagram. The maximal correlation between the streak function and the actual Hovmöller data was then recorded. Based upon our review of numerous cases in both radar animations and Hovmöller diagrams, a correlation threshold of 0.35 was subjectively found to discriminate best between coherent convective episodes and other disorganized convection. Contiguous swaths of correlations exceeding 0.35 were identified as "convective episodes," provided that they were at least 100 km in length and 3 h in duration [i.e., the MCS criteria of Parker and Johnson (2000)]. For the purposes of computing episode spans and durations, the starting and ending

[4] The 2° length setting represents a decrease from the 3° length used by Carbone et al. (2002). The effect of this shorter streak function is to define more precisely the starting and ending points of the precipitation episodes. Longer streak functions [cf. Carbone et al. (2002), who considered settings as large as 12°] would emphasize the motions of larger-scale envelopes of precipitation systems, including possible gaps wherein storms may dissipate and reform. Because convection is often widespread during warm-season days in the southeastern United States, we opted for a conservative approach that reliably separated seemingly unrelated groups of storms.

points were considered to occur at the first and last times that the correlation exceeded the 0.35 threshold.

Together, the two viewpoints show the long-term patterns of convective storms as well as the properties of the transient systems that make up those patterns. Additional details about our analysis methods are included as the data are presented in the next two sections.

3. Mean spatial and temporal structures

The mean storm frequency (Fig. 2) reveals that storms were most frequent along the Atlantic and Gulf coasts, and especially over the Gulf Stream just off the Carolinas. As discussed by Parker and Knievel (2005), there is a general decrease in Pr_{storm} toward the north, although the Tennessee and Ohio Valleys appear to have somewhat enhanced local storm frequencies for their latitudes. Poorer radar coverage partly accounts for the decrease in Pr_{storm} offshore beyond roughly 2° longitude from the coastline, as well as in western North Carolina and northern Virginia, where partial beam blockage is a problem. Indeed, Maddox et al. (2002) mapped in detail the radar coverage of the WSR-88D network, and showed that at 3 km MSL there are a few radar holes along the Appalachians (their Fig. 4a); the coverage at 5 km MSL is continuous (Maddox et al. 2002, their Fig. 4b), but radar beams may occasionally overshoot the 40-dB*Z* cores of some storms, leading to misses in the NOWrad composite. A few anomalous pixels also exist elsewhere (e.g., in northern Ohio and throughout New York), but for the most part the study domain (parallelogram in Fig. 2) did not possess large areas of suspiciously high or low values.

To assess the hypotheses that motivated this study, it was necessary to quantify the daily evolution of storms across the region. If convective systems develop over the Appalachian Mountains and move eastward, it would not be apparent from simple long-term averages such as in Fig. 2. The averaged Hovmöller diagram for the study period (Fig. 3) reveals that by far the predominant signal in the dataset is that of the well-known afternoon maximum in convection. This diurnal maximum appears (around 2100 UTC) at virtually every longitude between 88° and 74°W. During the nighttime hours (roughly 0300–1500 UTC) as the land surface cools, convection is suppressed over the elevated terrain and is maximized offshore over the Gulf Stream (east of 74°W; cf. Figs. 3 and 4). This late night–early morning maximum in offshore convection in the Southeast has been discussed by Lericos et al. (2002), who attributed it to the warm waters of the Gulf Stream,

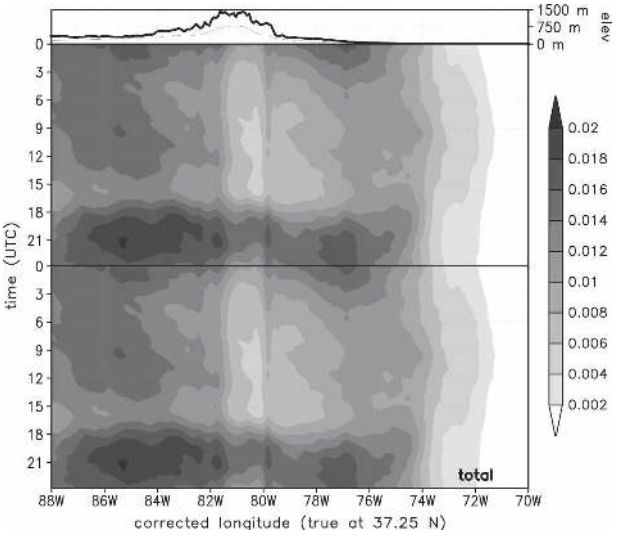

FIG. 3. Daily Hovmöller diagram of 9-yr mean Pr_{storm} for the window shown in Fig. 1. Hovmöller diagram is repeated to aid in the interpretation of features that overlay the change of day. The latitudinal maximum (thick) and mean (thin) surface elevations for the domain are shown for reference above.

nocturnal land breezes, and also convective systems that moved offshore late in the day. The final feature in Fig. 3 is a secondary maximum in storm frequency that occurs to the west of the Appalachians between roughly 0600 and 1500 UTC. This second peak corresponds to what Carbone et al. (2002) called the "semidiurnal signal between the (Rocky and Appalachian) cordilleras"; it represents nocturnal convective systems that enter the western edge of our study domain from the central United States (discussed in more detail later).

Although there is a slight suggestion of eastward-moving convective systems in Fig. 3, the amplitude of the primary diurnal maximum is so large that it generally masks any other signals in the southeastern United States. The time of maximum storm frequency is almost the same for every on-land pixel in the study domain (Fig. 4, bottom-right panel). This afternoon maximum corresponds to the leading empirical orthogonal function (EOF) of the Pr_{storm} dataset (Fig. 5a); it is strongly maximized at 2100 UTC, and accounts for 69.2% of the variance in Pr_{storm} (Fig. 5b). As shown in Fig. 6a, this daily signal is strongest over the far southeastern United States. Within the study domain, it is strongest along the North Carolina coast and over the Appalachian Mountains. There is almost no correlation to EOF1 in the Midwest, where nocturnal convective systems are frequent [echoing the findings of Wallace (1975)], and there is anticorrelation offshore, especially where the warm Gulf Stream waters pass near the coast of the Carolinas.

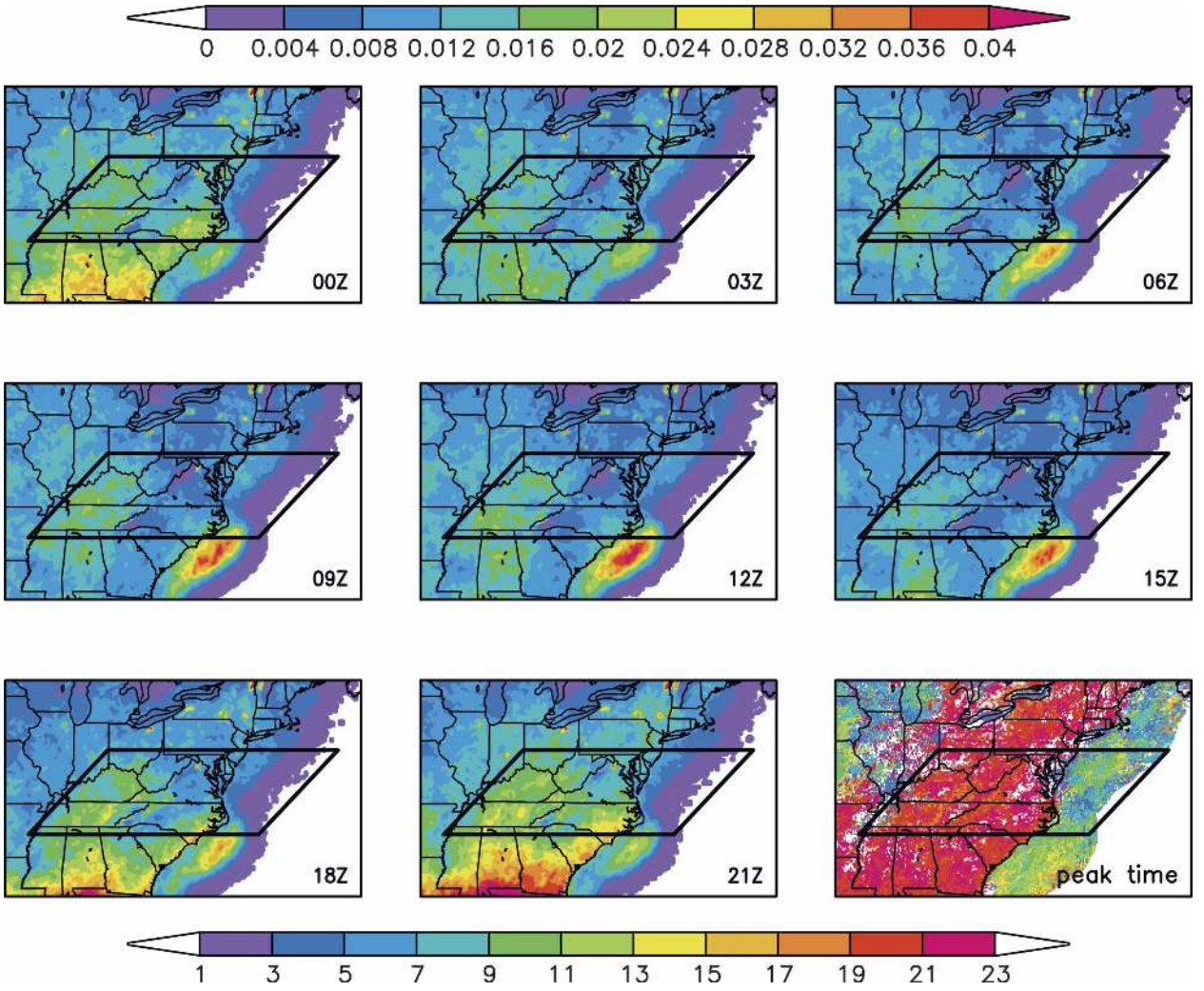

FIG. 4. Maps of 9-yr mean Pr_{storm} at 3-hourly intervals, shaded as shown at top. The time of maximal Pr_{storm} is depicted in the bottom-right panel, shaded as shown at bottom. In each panel, the window for the longitude-shifted Hovmöller diagrams (Fig. 3, etc.) is outlined by a parallelogram.

The first four EOFs appear to dominate the variability (Fig. 5b), and because the extrema of their coefficients are out of phase from one another (Fig. 5a), they are likely to contain whatever patterns of recurring, propagating convective systems exist within the dataset. The second EOF is maximized around 1800 UTC and minimized around 0200 UTC (Fig. 5a); in other words, it represents the local earliness or lateness of convection relative to the principal afternoon maximum around 2100 UTC. As seen in Fig. 6b, the diurnal maximum in storms is comparatively early (loadings >0) along the coasts, the Appalachian Mountains, and the Cumberland Plateau in eastern Tennessee; it is comparatively late (loadings <0) over the Piedmont and coastal plain. In other words, the spatial loading map of EOF2 is consistent with convection that develops over the higher terrain and then moves eastward off the Appalachians. The third EOF has peaks in the late afternoon, as well as during the early morning (Fig. 5a); it is strongly maximized offshore and weakly maximized over the Tennessee and Ohio Valleys (not shown), and appears to represent locations that have a secondary maximum in storms at night, as well as a delayed afternoon maximum. The fourth EOF (Fig. 5a) appears to represent locations with an early afternoon maximum in storms, but also a few nighttime storms; accordingly, it is maximized over the eastern and western slopes of the Blue Ridge and weakly along the coast (not shown).

The first EOF is so predominant (spatially and in terms of variance) that, even if it is not the pure diurnal cycle, it must be very heavily weighted toward it. Certainly, if there is recurring propagating convection in

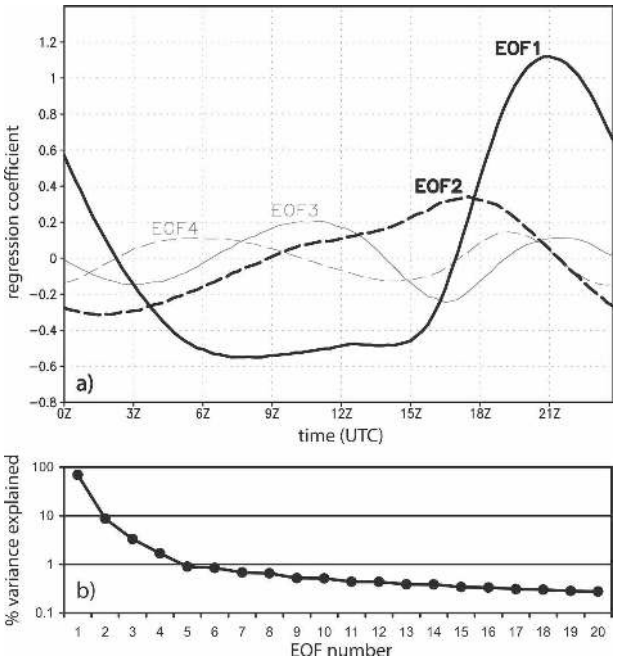

FIG. 5. (a) Diurnal cycle of coefficients for the first (thick solid), second (thick dashed), third (thin solid), and fourth (thin dashed) EOFs, and (b) the percent of variance explained by the first 20 EOFs for the 9-yr Pr_{storm} dataset.

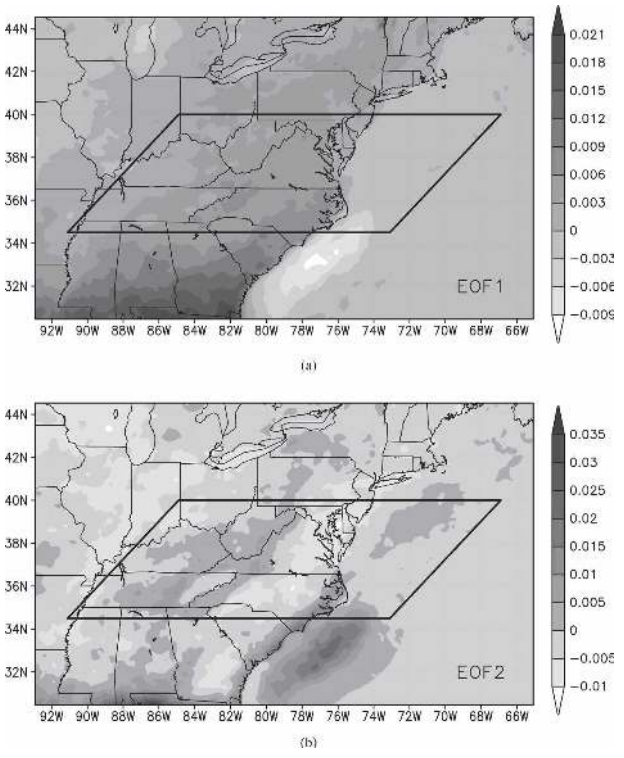

FIG. 6. Maps of the loadings for (a) the first and (b) the second EOFs describing the 9-yr Pr_{storm} dataset. The units are those of fractional storm frequency (cf. Fig. 2).

the region, then some aspect of it is likely included within EOF1 as well. However, in trying to depict such behavior more clearly, we removed the signal of EOF1 from the dataset (Figs. 7 and 8), in order to reveal synoptic and mesoscale precipitation episodes that otherwise would be completely overwhelmed by the daily afternoon peak in storms.

Non-EOF1 convective initiation is maximized around 1800 UTC over the coast (Fig. 8, and around 75°W in Fig. 7) and the eastern Blue Ridge front (Fig. 8, and around 81°W in Fig. 7), whereas at this time storms are suppressed over the Piedmont and coastal plain (Fig. 8, and from 76° to 80°W in Fig. 7). This minimum may be attributable to the frequent lack of an adequate local lifting mechanism (as compared to the elevated terrain to the west and the coastal sea-breeze front to the east); even when mesoscale boundaries are present over the region (e.g., Koch and Ray 1997), there is likely to be some time lag relative to higher locations, which almost certainly reach their convective temperatures first. Our idealized model simulations (not shown) also suggest that very weak subsidence may extend downstream of the Appalachians by as much as 300 km [much as in the mountain–plains solenoid of Wolyn and McKee (1994)], which could stabilize the environment at lower elevations and delay convection (cf. Tripoli and Cotton 1989).

Finally, the later maximum in storms may include the signal of convective systems that develop over the Appalachians or the coast and then move into the region. The time of maximal non-EOF1 storm occurrence over the Piedmont–coastal plain is around 0000 UTC (Fig. 8, bottom-right panel) and this maximum appears to be connected to the earlier Appalachian and coastal maxima via swaths of enhanced Pr_{storm} (Fig. 7: streak e, speed $= -5$ m s^{-1}; streak g, speed $= 9$ m s^{-1}). This "connection," along with the basic progression[5] from 1800 UTC through 0300 UTC in Fig. 8, supports the possibility of recurring convective systems that move into the Piedmont and coastal plain from the east and the west.

Many of the patches of maximized Pr_{storm} in the residual Hovmöller diagram (Fig. 7) slope eastward in time, with characteristic speeds ranging from 10 to 20 m s^{-1}. Convective systems that enter the domain from the west at night are particularly evident in Fig. 7

[5] The progression is somewhat masked at 2100 UTC in Fig. 8 because the maximum just east of the Blue Ridge front at 2100 UTC (cf. Fig. 4) is in phase with the regional daily peak, and hence it is largely removed when EOF1 is removed.

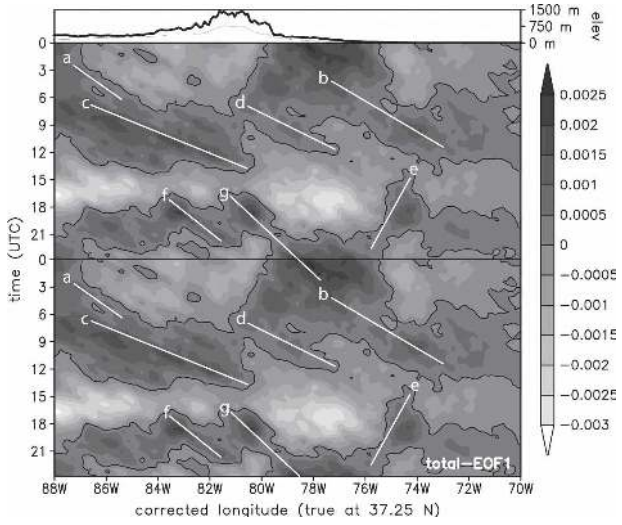

FIG. 7. Same as in Fig. 3 except that the residual Pr_{storm} after the first EOF (the mean afternoon maximum in storms; cf. Figs. 5 and 6a) has been removed. Values are shaded as shown, with the 0 level contoured for emphasis. The white line segments correspond to streaks identified by the algorithm of Carbone et al. (2002), and are labeled for reference in the text. Note that for this figure, the episode detection algorithm was modified slightly from what is described in section 2: the length of the correlation function was decreased from 2° to 1.33° longitude, and the minimum threshold for the correlation function was increased from 0.35 to 0.375. These changes had the effect of identifying only longer and more distinct streaks; they were needed because the long-term averages in this figure have broader and more diffuse maxima than the individual case days did.

(streak a, speed = 12 m s^{-1}; streak c, speed = 20 m s^{-1}). Figure 8 supports the idea that such systems most frequently arrive from the northwest (the maxima over Illinois–Ohio at 0300 and 0600 UTC). It is of interest that the signals of streaks a and c in Fig. 7 appear to arrive at the Appalachian chain around 1500 UTC, that is, just before the onset of convective development the next day. There is also the suggestion of another swath of Pr_{storm} connecting convection over the Piedmont–coastal plain between 0000 and 0600 UTC to convection over the Gulf Stream around 0900–1200 UTC (Fig. 7: streak b, speed = 14 m s^{-1}). This is less evident in the spatial maps (Fig. 8), which may mean that most convective episodes over the coastal plain dissipate by 0600 UTC, whereas a minority move offshore and reintensify. As mentioned above, the semidiurnal offshore maximum is more strongly linked to the preference for nighttime convection over the warm waters, possibly with some contribution from triggering by land-breeze fronts.

Several other smaller features include the signature of convection that develops over the Cumberland Plateau and moves eastward (Fig. 7: streak f, speed = 11 m s^{-1}), and a more mysterious streak extending eastward from the Blue Ridge at night (Fig. 7: streak d, speed = 17 m s^{-1}). This latter signal (streak d) partly appears to be an artifact that is introduced when EOF1 is removed, and it arises because the afternoon maximum in convection over the Appalachians is greater in amplitude than is the nighttime minimum. The data for individual convective episodes (next section) do not show a secondary maximum in convective development over the Blue Ridge at night. Overall, a daily maximum around 2100 UTC is predominant in the eastern United States. However, once this diurnal maximum is removed, most of the streaklike signatures appear to fit with a conceptual model that includes moving convective systems through the eastern Piedmont and coastal plain during the afternoon and evening hours.

4. Individual convective episodes

Motivated by the encouraging results from section 3, we sought to identify convective episodes using the techniques employed by Carbone et al. (2002) and Ahijevych et al. (2004). In all, this technique identified 2128 convective episodes over the 9-yr period (236 yr^{-1}). Although not as intense as many MCSs in the central United States, the episodes were still persistent. On average, the episodes lasted for 6.3 h and spanned 302 km; roughly half of the episodes (1093, or 121 yr^{-1}), had spans longer than 250 km. Most of the episodes (1945, or 91%) moved eastward with time, having an average speed of 14 m s^{-1}. The remaining 183 (9%) moved westward with time, having an average speed of −11 m s^{-1}.

Roughly one-quarter (543) of the identified episodes originated outside of the study domain and entered it from the west. Much as emphasized by Carbone et al. (2002) for the central United States, the impact of propagating convective systems is an important part of the eastern U.S. climatology. In other words, short-term forecasts of thunderstorms and precipitation in the eastern United States are more complicated than the simple local diurnal cycle.

Discounting those systems that entered the domain from the west (leaving 1585 "interior" systems), most of the episodes began between 1600 and 2000 UTC, with the longer-spanning episodes having an earlier start (Fig. 9a). Most of these interior episodes then dissipated between 2200 and 0600 UTC, with the longer-spanning episodes having later ending times (Fig. 9a). It is unsurprising that the systems that were longer lived (started earlier in the day and ended later in the day) tended to travel over greater longitudinal spans. The more important finding is that most of the eastern U.S.

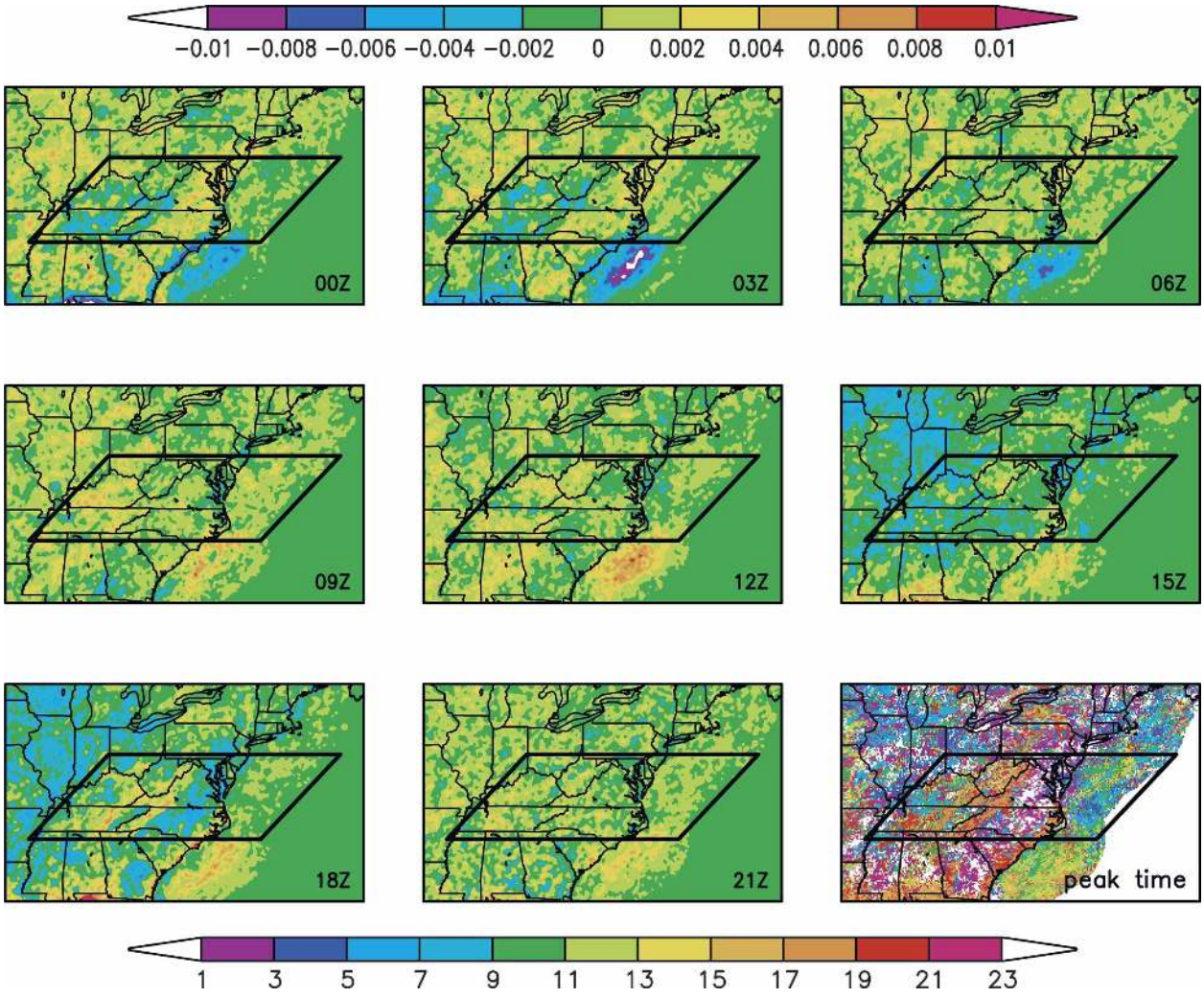

FIG. 8. Same as in Fig. 4 except that the residual Pr_{storm} after the first EOF (the mean afternoon maximum in storms; cf. Figs. 5 and 6a) has been removed.

episodes developed in the afternoon and survived into the evening hours; this result meshes well with streaks e–g in Fig. 7. This afternoon–evening cycle in frequency is reminiscent of that which occurs over the Rocky Mountain Front Range and the high plains of the central United States. However, the eastern episodes are not only generated in the afternoon: out of the 1585 total episodes, at least 80 developed in each 2-h window throughout the day and night (Fig. 9a).

Beyond the gross statistics of the population of convective episodes, it is worthwhile to consider the properties of the eastward movers and westward movers in turn. This subdivision provides a clearer depiction of the kinds of convective systems that make up the objectively identified "episodes" dataset, and their typical patterns of movement.

a. Eastward-moving episodes

Among the interior convective episodes, 1402 (88%) moved eastward in time. Development of eastward movers was maximized in two locations: over the eastern slopes and foothills of the Blue Ridge Mountains (79°–80°W; Fig. 9b), and over the western part of the study domain (85°–86°W; Fig. 9b).

1) DEVELOPMENT NEAR THE BLUE RIDGE

Systems developing over the Blue Ridge Mountains and foothills tended to decay within 1°–2° longitude of the coast (Fig. 9b). The shoulder of the maximum in initiation is broad and extends eastward across the Piedmont, suggesting that the large maximum around 0000–0300 UTC in Fig. 7 includes both systems that

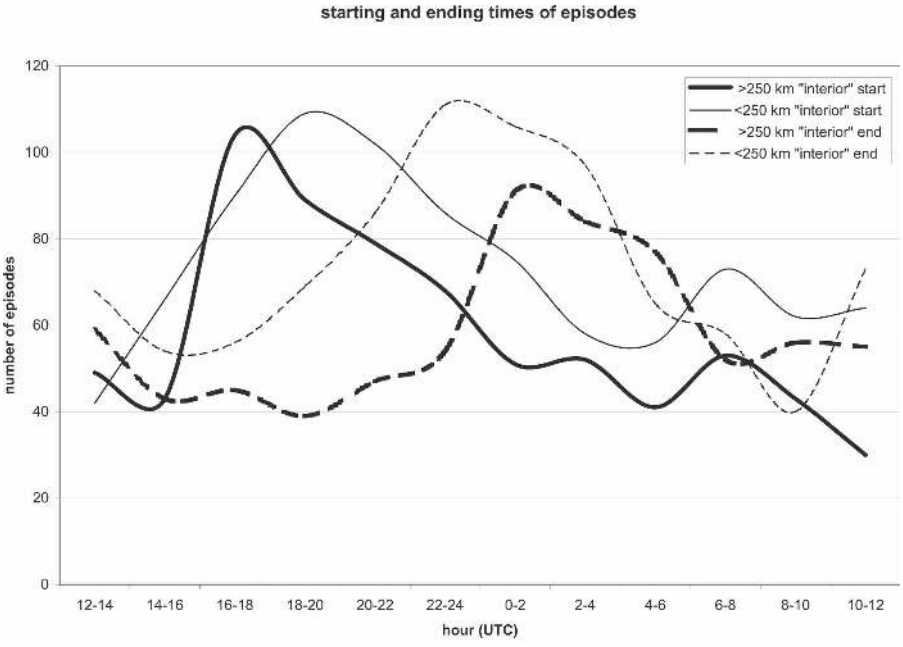

(a)

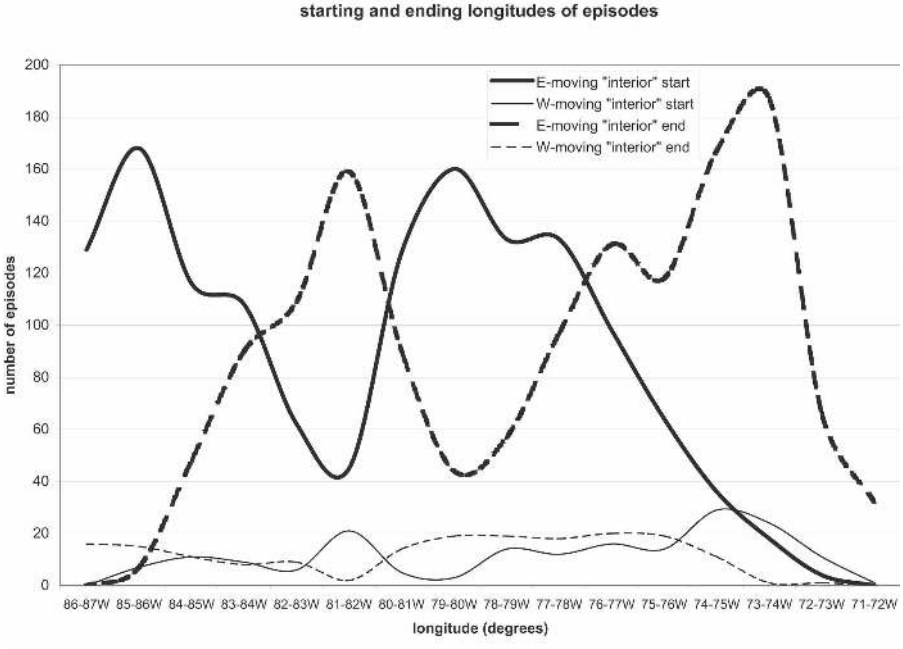

(b)

FIG. 9. Total number of identified convective episodes that began within the study domain (i.e., did not enter through the boundary of the domain) in terms of (a) starting and ending times, for both large and small episodes, and (b) starting and ending "corrected longitudes" (true at 37.25°N) for both eastward- and westward-moving episodes.

TABLE 1. Fraction of eastward-moving episodes that survive to the east of 80°W (i.e., to the east of the Blue Ridge front), and to the east of 76°W (i.e., to the east of the Atlantic coast).

Episode starting point	No. of episodes	% surviving east of 80°W	% surviving east of 76°W
West of 87°W (entering domain)	543	6.8	3.3
84°–87°W (west of Cumberland Plateau)	426	10.1	3.1
82°–84°W (Cumberland Plateau)	160	29.4	11.9
80°–82°W (Blue Ridge)	187	96.3	32.6
78°–80°W (Piedmont)	296	N/A	52.0
76°–78°W (coastal plain)	216	N/A	95.4
East of 76°W (offshore)	117	N/A	N/A

have moved into the region from the west (e.g., streak g) and episodes that developed locally over the Piedmont. The fact that such a large number of eastward-moving episodes do not decay until 73°–74°W (Fig. 9b) supports the interpretation of streak b in Fig. 7 as the footprint of convective systems.

Although the detection algorithm separates streaks b and g in Fig. 7, it is not hard to envision that part of this signal results from convective episodes that move all the way across the region, from the Blue Ridge foothills through the coastal zone. Roughly one-third of the identified episodes beginning over the Blue Ridge made it past 76°W (i.e., through the coastal plain), and roughly half of the episodes beginning over the Piedmont made it to the coast (Table 1). From Figs. 7 and 9 and Table 1, the integrated picture is of convective systems that develop over the higher terrain of the Blue Ridge and the Piedmont, then move eastward, often as far as the coast.

An example of one such episode from 11 to 12 July 2003 is depicted in Fig. 10 (along with the streak identified by the automated algorithm). A time series of reflectivity (Fig. 11) illustrates the evolution of this case, with storms developing over the eastern front of the Blue Ridge around 1800 UTC, their subsequent organization into a squall line of moderate intensity, and continued movement to the coast through 0200 UTC. The system subsequently decayed, although there were other cases (not shown) in which the episodes survived until they were farther offshore. We have not performed a detailed study of the possible interactions, but the fact that convective episodes may move offshore after midnight has interesting implications for the regeneration of nocturnal storms off the Carolina coasts (where the Gulf Stream is quite close to the shore).

Eastward-moving convective episodes that develop over the high terrain and move down the slope are at least qualitatively similar to those that occur in the central United States. Future studies should consider whether the governing processes are also similar. The eastern U.S. "afternoon–evening convective episodes" mode could be relatively simply explained by the afternoon orographic thermal forcing, followed by subsequent advection by the prevailing westerlies and generation of cold thunderstorm outflows that descend the slope and lift the warm, moist boundary layer that is common over the southeastern United States. Other, much more sophisticated, mechanisms have been proposed for the genesis and maintenance of convective systems in the central United States (e.g., Tripoli and Cotton 1989). It may be that those additional processes, especially the presence of nocturnal low-level jets, account for the greater size and longevity of MCSs in the

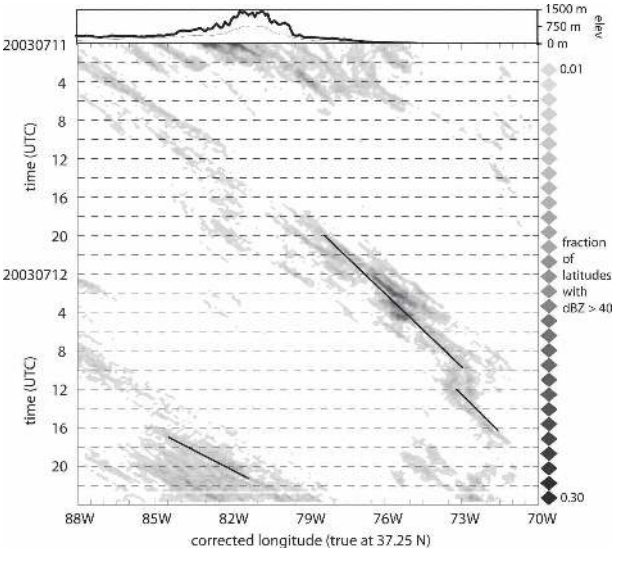

FIG. 10. Hovmöller diagram of observed latitudinal Pr_{storm}, shaded as shown, for a case characterized by episode development over the Blue Ridge on 11–12 Jul 2003 (cf. Fig. 11). A Pr_{storm} of 0.25 corresponds to a pixel ≥40 dBZ at 25% of the latitudes within the window shown in Fig. 1. The latitudinal maximum (thick) and mean (thin) surface elevations for the domain are shown for reference above. Episodes identified by the streak detection algorithm are represented by black line segments that connect their starting and ending times (cf. section 2); during its lifetime, a system's speed may deviate from this simple line.

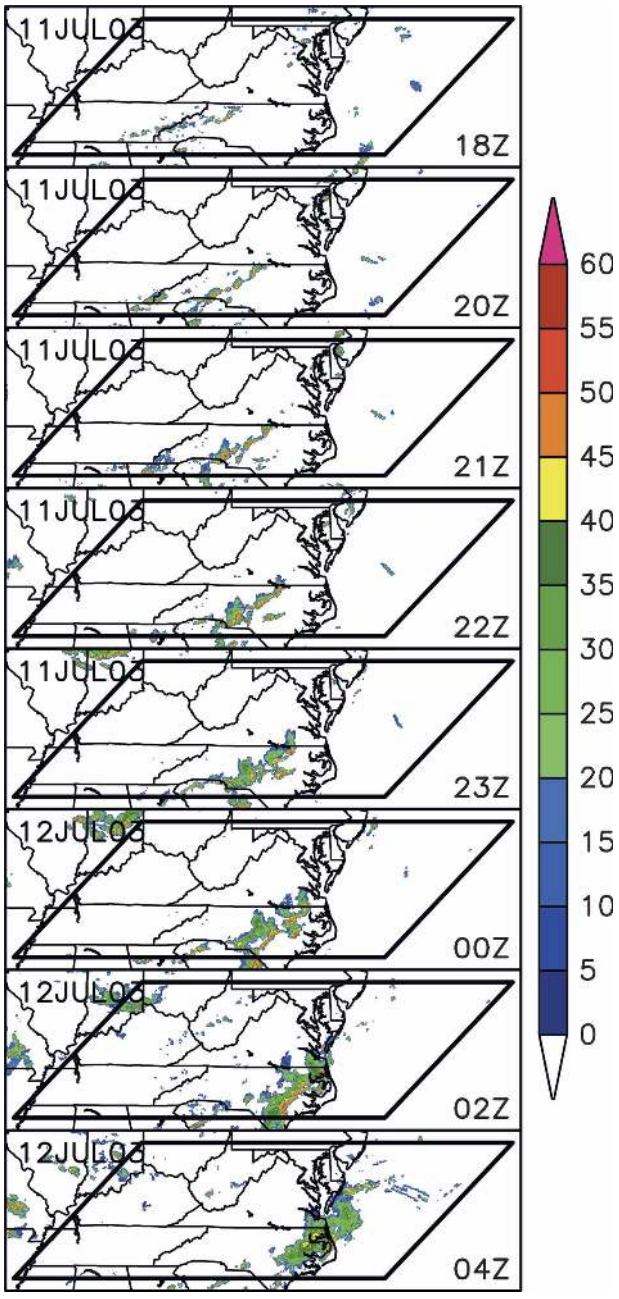

FIG. 11. Composite radar reflectivity (dB*Z*, color shaded as shown) for 11–12 Jul 2003, at eight of the times included in the Hovmöller diagram in Fig. 10a. The parallelogram denotes the window over which the latitudinal Pr_{storm} was computed in Fig. 10.

central United States. Other features, such as the persistent west-to-east slope of the high plains, and the frequent presence of potential instability due to elevated, dry, well-mixed layers over the central United States may also play a role. In any case, the delayed diurnal maximum downstream of the high terrain remains in the eastern United States, and long-lived convective systems appear at least partly to contribute to it.

2) EPISODES CROSSING THE BLUE RIDGE

A large fraction of the eastward movers that developed west of the Appalachians ended before they crossed the Appalachians, with a maximum in dissipation on the western slope of the Blue Ridge (81°–82°W; Fig. 9b). In fact, only 7% of the episodes that entered the domain from the west, and only 10% of the interior episodes that began west of the Cumberland Plateau, survived to the other side of the Blue Ridge (Table 1). A much larger fraction of the episodes that began over the Cumberland Plateau survived all the way across the Blue Ridge, and almost all of those that began over the Blue Ridge survived to its east (Table 1). Of course, this result is less meaningful because when Blue Ridge storms dissipated before departing the mountains, their Hovmöller streaks would normally be too short to be identified as an "episode" in this study.

Although episodes dissipated much more frequently than they crossed the Appalachians, during the study period 127 systems (14 yr^{-1}) starting west of 82°W were able to complete the journey (derived from Table 1). Despite the fact that streaks c and g do not connect in Fig. 7, the successful crossings were most likely when episodes approached the Appalachians around the time of the local diurnal maximum (i.e., the window from 1700 to 2200 UTC). Such phasing is not uncommon, and is loosely depicted in the long-term-averaged Hovmöller diagrams of Carbone et al. (2002). One such example occurred on 17–18 June 2000 (Figs. 12 and 13).

Storms developed in the late morning hours along the western edge of the higher terrain in West Virginia, Kentucky, and Tennessee (in the vicinity of a stationary front: not shown) and moved eastward through 1700 UTC (Fig. 13). As of 1900 UTC, the primary episode had the signature of a leading convective line with a small region of trailing stratiform precipitation (Fig. 13); meanwhile, other storms began to develop over the Blue Ridge in North Carolina and Virginia. By 2300 UTC, the original "western" episode was crossing the Blue Ridge, and had become somewhat disorganized, while the later-developing "eastern" episode of storms had moved into the North Carolina and Virginia Piedmont. This eastern episode was also detected by the objective algorithm, and is denoted by the shorter, right-hand line segment from 1800 to 2130 UTC in Fig. 13.

The western episode had finished traversing the Appalachians by 0100 UTC, with its northern part surviving into northern Virginia and Maryland, but with its southern part dissipating to the west of the eastern epi-

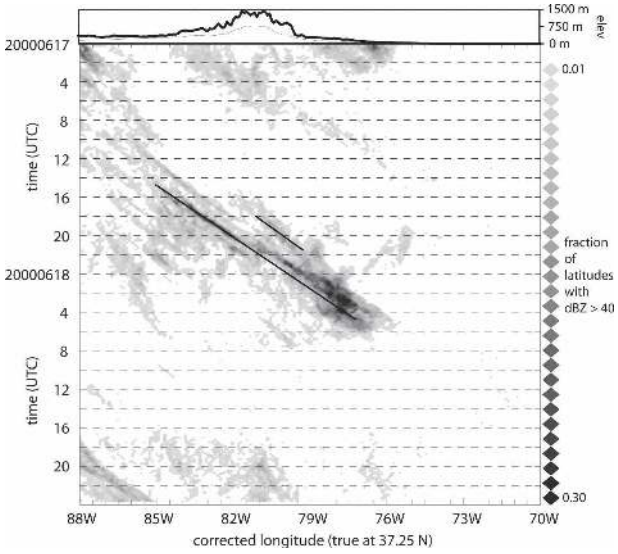

FIG. 12. Same as in Fig. 10 but for a case characterized by an episode crossing the Blue Ridge on 17–18 Jun 2000 (cf. Fig. 13).

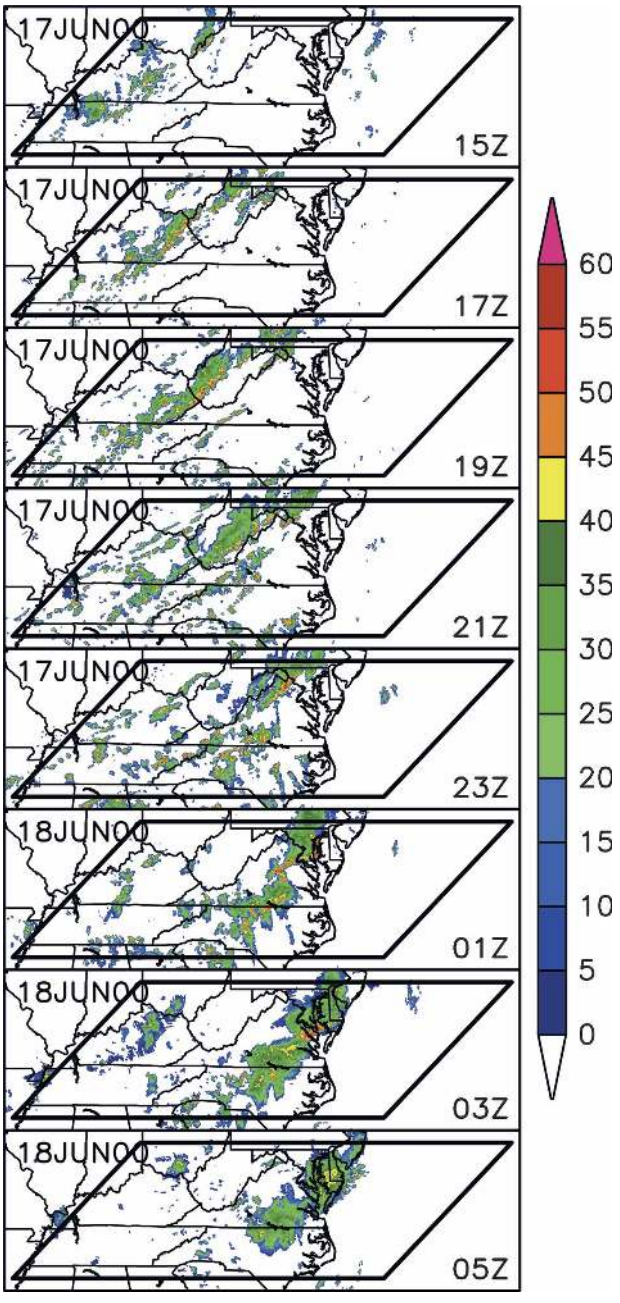

FIG. 13. Same as in Fig. 11 but for 17–18 Jun 2000, at eight of the times included in the Hovmöller diagram in Fig. 12.

sode over North Carolina and southern Virginia. Over the next few hours, the western episode caught up with and became parallel to the eastern episode (e.g., at 0300 UTC in Fig. 13), such that only one broad, intense swath (rather than two distinct streaks) was apparent in the Hovmöller depiction (Fig. 12). As in most eastern U.S. episodes (Fig. 9a), dissipation occurred around 0500 or 0600 UTC in the coastal zone. In general, most successful crossers in the dataset passed over the Appalachians around the time that convection was most favored there. However, in this case, the additional orogenic convection over North Carolina and Virginia may have consumed whatever instability was present over the southern part of the domain, meaning that only the northern half of the original convective system survived the traverse.

The concept of an Appalachian-crossing convective episode has aroused recent attention (Frame and Markowski 2006), and is of great interest to forecasters on the east side of the Blue Ridge (K. Keeter, NWS, Raleigh, NC; S. Keighton, NWS, Blacksburg, VA; L. Lee, NWS, Grier, SC; 2006, personal communication). Frame and Markowski (2006) emphasized the processes associated with the partial blocking of a squall line's cold pool of outflow by terrain. They suggested a replacement cycle in which the original convective line weakens while ascending the ridge's windward slope, while the cold pool initiates a new convective line on the ridge's lee side: after some of the outflow passes over the ridge, it descends the lee slopes rapidly within a supercritical flow regime, then undergoes a hydraulic jump and resumes deep lifting. In this regard, the time of day may again be important: the decreased low-level stability of the afternoon would hinder the cold pool less as it ascended the windward slope.

Within our 9-yr dataset, there were indeed occasions when convective systems dissipated on the western slope of the Appalachians, but then re-formed on the eastern slope. Our streak detection algorithm would not usually identify these as contiguous episodes (see footnote 4, above), so we have not been able to quan-

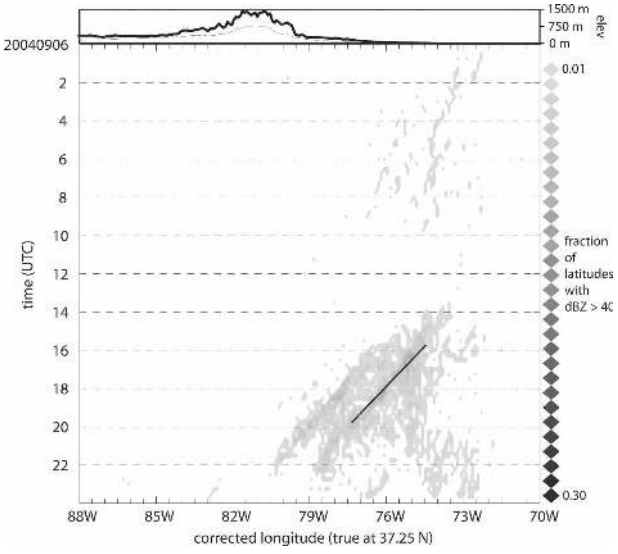

FIG. 14. Same as in Fig. 10 but for a case characterized by a westward-moving episode on 6 Sep 2004 (cf. Fig. 15).

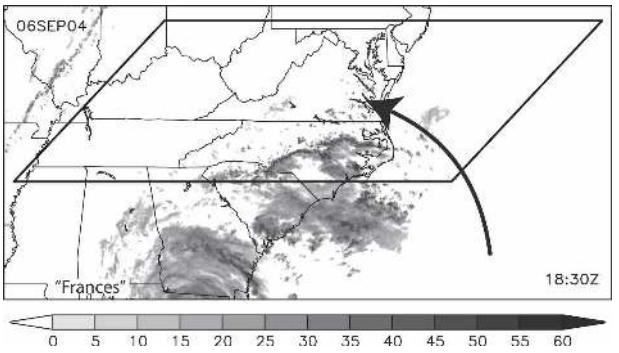

FIG. 15. Same as in Fig. 11 but for 1830 UTC 6 Sep 2004, one of the times included in the Hovmöller diagram in Fig. 14. Locations of Tropical Storm Frances and the general sense of the regional prevailing flow are indicated.

tify the frequency of this behavior. But, our finding that roughly 11% of all systems from the west cross the Blue Ridge is undoubtedly conservative, and likely underestimates the number of mesoscale regions of dissipating and reforming convection that can be loosely tracked across the mountains. Frame and Markowski (2006) noted that increasingly tall ridges more strongly favor the disruption and replacement cycle associated with the cold pool's passing over a ridge. Although they considered mountains as tall as 1800 m in their idealized framework, it still may be that the Blue Ridge is too tall for some cold pools to cross over. But, another intriguing possibility is that the potential vorticity (PV) anomalies generated by mesoscale regions of convective and stratiform heating may be advected over the terrain in the middle troposphere. Once on the lee side, if CAPE is present, the PV anomalies could then aid in redevelopment through processes such as described by Raymond and Jiang (1990) and Fritsch et al. (1994). Prior studies using 2D or quasi-2D model configurations would be unable to capture such an effect, so additional study is warranted.

b. Westward-moving episodes

Among the interior convective episodes, 183 (12%) moved westward in time. Development of the westward movers was maximized in two locations: over the western slopes and foothills of the Blue Ridge Mountains (81°–82°W; Fig. 9b) and over the Atlantic coast (74°–75°W; Fig. 9b). Their dissipation did not appear to be preferentially linked to any particular geographic features.

The formation of convective episodes along the coastline appears to correspond to streak e in Fig. 7, and would be associated with long-lived storms generated by the diurnal sea breeze, which subsequently moved inland. The formation of episodes on the western slope of the Blue Ridge would appear to be the counterpart to the maximum of the eastern slope. Westward movers would be favored in weak flow, when thermally driven convection develops over the higher terrain and then convective outflows provide continual retriggering of new storms as they move downslope toward the west.

Interestingly, however, when we took a closer look at the longest-lived westward movers with the greatest longitudinal span, we found that many of them were associated with landfalling tropical cyclones (TCs). Particularly when TCs approached the study domain from the south, the prevailing easterly flow across the study domain, paired with onshore advection of warm moist air and the presence of TC rainbands, led to westward-moving convective episodes. An example of one such episode from 6 September 2004 is depicted in Fig. 14 (along with the streak identified by the automated algorithm). Absent other information, the Hovmöller depiction gives the impression that this may be inland-moving sea-breeze convection (developing near the coast), but the regional reflectivity data (Fig. 15) reveal that these are bands of convection embedded within the easterly flow in advance of Hurricane Frances. We found many westward movers that were not associated with TCs, but some of the longest-lived examples arose from this kind of scenario.

c. Annual distribution and relationship to wind shear

Although the eastern United States is not commonly thought to have large numbers of organized convective

systems, their signals are evident once the principal afternoon maximum is removed from the long-term dataset, and an episode identification algorithm reveals that there are hundreds each year. A final question concerns the environmental factors that might support organized convection and their distribution throughout the year in the study domain. Clearly, instability is required for convection; numerous studies (e.g., Rotunno et al. 1988) have also shown that at least a modest amount of vertical wind shear favors long-lived, organized convective systems.

The annual distribution of convective episodes in the study domain peaks in midsummer (Fig. 16a), when instability is at its annual peak in the southeastern United States; the mean lifted index[6] for an episode was most negative in June–August, with a minimum of −3.4°C in July. However, the midsummer peak in frequency also coincides with the annually minimized vertical wind shear (Fig. 16a), due to the general lack of summer baroclinicity in the region.

The annual frequency maximum in July holds true for all subsets of the data except for those systems entering the domain from the west, which are maximized in May. It may be that the severe, long-lived squall lines that traverse much of the central United States do require more shear [e.g., those studied by Coniglio et al. (2006)], such that their numbers decrease by midsummer when the midlatitude shear is smaller. Long-lived, intense MCSs in the central United States often occur in environments with vertical wind shear exceeding 5×10^{-3} s^{-1} throughout much of the troposphere (Coniglio et al. 2006). However, the minimal threshold for organized convective systems is probably smaller: perhaps a mean value of 2.5–3 $\times 10^{-3}$ s^{-1} in the lower and middle tropospheres (M. Coniglio 2006, personal communication), or, based on a climatology from the North American Monsoon Experiment,[7] even as low as 1.5×10^{-3} s^{-1} (R. Carbone 2006, personal communication).

Despite the smaller shear during the season of peak frequency, 90% of the convective episodes in our study occurred within environments that had at least 2.5×10^{-3} s^{-1} of bulk shear in the surface–700-hPa layer (Fig. 16b). Even in the lowest-shear month (August), the mean surface–700-hPa bulk shear for episodes was 3.7×10 s^{-1} (Fig. 16). This value is actually above the median annual value for all soundings (Fig. 16b), suggesting that even though instability is usually present in the southeastern United States during the summer, organized convective episodes only occur on days with relatively higher shear. The values of surface–500-hPa shear are lower, suggesting that most of the vertical wind shear on days with episodes is present in the lower troposphere. This fits with the conceptual model of Rotunno et al. (1988), which emphasizes the importance of the lower-tropospheric shear. Even so, 90% of the convective episodes occurred in the surface–500-hPa bulk shear exceeding 1.7×10^{-3} s^{-1}, and the mean value in August was 2.5×10^{-3} s^{-1} (again, above the median for all soundings; Fig. 16b).

The summertime values for shear over the central United States[8] are definitely higher, with averaged August surface–700-hPa bulk shear of 3.1×10^{-3} s^{-1} and surface–500-hPa bulk shear of 2.2×10^{-3} s^{-1}. But, although smaller, the vertical wind shear over the eastern United States was adequate. When convective episodes occurred in our study period, vertical wind shear usually exceeded the experts' estimated thresholds for convective systems (reported above), even for deeper layers during the summer months. A principal finding is that, despite our initial skepticism, sufficient vertical wind shear to support organized convective systems is frequently present in the southeastern United States during the summer months. The frequency of convective episodes appears to be linked to the cycle of conditional instability and is maximized in the summer. However, most of the convective episodes occurred in above-average (for the region) vertical wind shear: its importance to organized convection is supported by our dataset. Notably, other recent studies (Tuttle and Carbone 2004; Tuttle and Davis 2006) have also shown that, although requiring some CAPE, episodes are more strongly linked to enhanced vertical wind shear.

The annual distribution of organized convective episodes meshes nicely with the climatological maximum of severe winds in the study domain, which extends from May through August and peaks in July (Doswell et al. 2005). One forecaster with whom we shared these results wondered whether the episodes moved faster during the peak severe wind months, as faster convective systems have a greater likelihood of producing strong surface winds [owing to the additive effect of the storm motion; e.g., Evans and Doswell (2001)]. We find that there is no systematic annual variation in system speeds, though there is a slight tendency for faster systems in the spring (the highest mean was for May, at

[6] The lifted index and vertical wind shear values were computed using the routine operational rawinsonde sounding that was nearest in space and time to an episode's starting point.

[7] This climatology was for convective episodes within a tropical regime possessing a lower-tropospheric easterly jet.

[8] The central U.S. shear values were computed using all of the soundings for the study period from Norman, OK; Springfield, MO; Topeka, KS; Omaha, NE; Davenport, IA; and Aberdeen, SD.

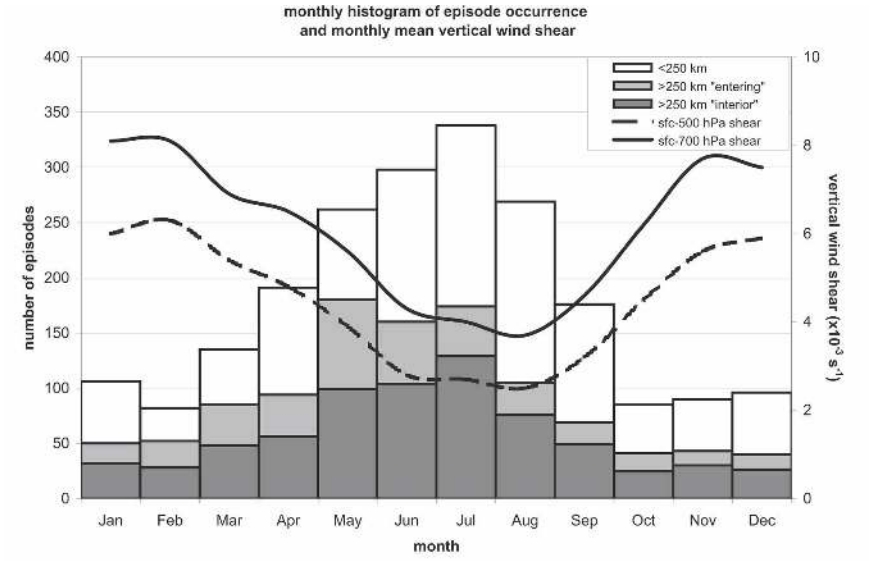

(a)

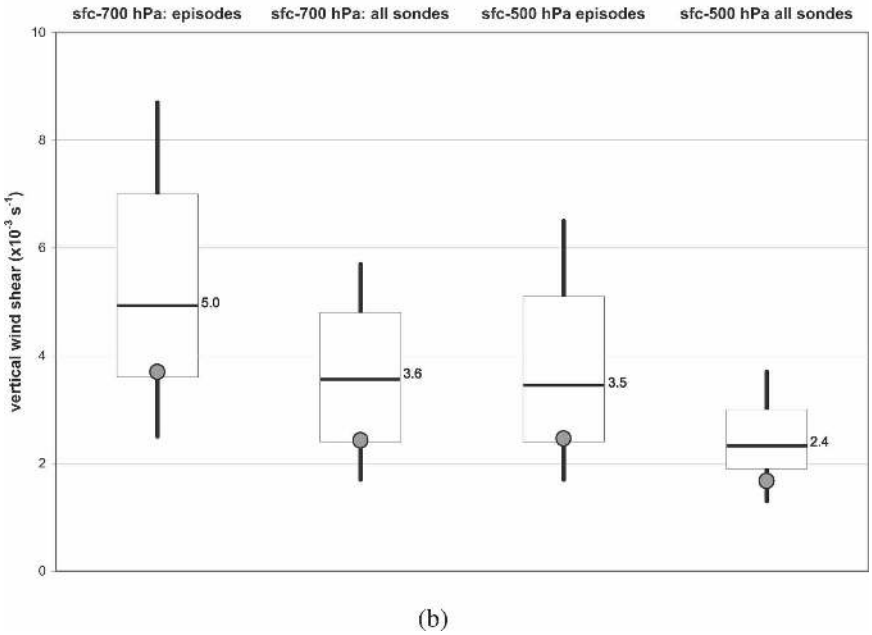

(b)

FIG. 16. Relationship of identified convective episodes to vertical wind shear: (a) annual distribution of episodes (columns) and their mean environmental shear (curves) in the surface–700-hPa and surface–500-hPa layers; the episodes are divided into small systems, large systems that enter the western edge of the domain, and large systems that begin within the domain. (b) Box and whiskers plots of the mean-layer shear in the surface–700-hPa and surface–500-hPa layers, both for the identified convective episodes and for every sounding during the study period. The boxes bound the middle two quartiles of the population, with the median shown as a dark line. The whiskers extend to the 10th and 90th percentiles. The gray circles in (b) indicate the population mean values for Aug (the month with the lowest mean shear). The vertical wind shear for the episodes was computed using the routine operational sounding nearest to the starting point of the episode. The mean environmental shear was computed by averaging all of the soundings from the region (Greensboro and Morehead City, NC; Roanoke, Wallops Island, and Washington–Dulles, VA; Nashville, TN; and Wilmington, OH) for each month.

17.6 m s^{-1}) and slower systems in the fall (the lowest mean was for September, at 11.1 m s^{-1}). However, there were also peaks in speed in February and October, and the maximum in May is largely attributable to the greater fraction of systems that enter the domain from the west (e.g., Fig. 16a). In any case, these peaks in storm speed do not phase with the late June/early July maximum in severe winds over the study domain. Our interpretation is that the greater number of convective episodes is what accounts for the peak in severe wind reports.

5. Statistics for summer months

As mentioned in section 2, we analyzed full years' worth of data because convective storms occur in our study domain during every month. Even so, it is probable that the mechanisms for initiating convection vary between the winter and summer months. In particular, convective forcing during the cold season is more likely to be associated with fronts and cyclones that move through the region. In such regimes, the development of convection is less strongly linked to the diurnal cycle, and the speeds of convective episodes are largely dictated by the translation speeds of the synoptic-scale systems that produce them. It is also possible that radar bright bands associated with melting snow were present in the Pr_{storm} field during the winter months; bright bands likely would not be identified by the streak detection algorithm, but might subtly influence the mean diurnal cycle of storms. In an attempt to determine the degree to which cold season systems might be influencing our results, we isolated the months of June–August (JJA) for further analysis. These 3 months were the lowest in terms of vertical wind shear (Fig. 16a), such that the influence of large-scale baroclinic systems would be at its annual minimum.

Because the JJA episodes represented 43% of the total population, it is probably not surprising that their mean statistical properties were similar to those of the full-year dataset. The mean durations of episodes did not vary significantly throughout the year, with the longest-lived systems (6.8 h) occurring in September and October and the shortest-lived systems (5.7 h) occurring in January; the average JJA system's lifetime was the same as the annual mean. However, throughout the course of the summer months, the span of convective episodes was somewhat shorter, decreasing from a peak in May of 381 km to a minimum in September of 262 km. In short, summer episodes traversed smaller distances despite their comparable lifetimes, presumably due to diminished middle- and upper-tropospheric winds.

Although JJA episodes detected by the objective algorithm had similar statistics to the overall population, we wondered if the signals of diurnally generated storms and propagating episodes would be clearer in our mean spatial and temporal reflectivity patterns once the "noisy" cold season months were removed. We recomputed the EOFs (described in sections 2 and 3) for the JJA-only data, and compared them to our full-year analyses. In terms of their timing and shape, the diurnal cycles for the leading EOFs in JJA were almost identical to those shown for the full year in Fig. 5a; the difference was that the amplitudes were approximately three times higher for JJA. Thus, even if there were *no* storms during the remaining 9 months of the year, the storms from JJA alone would be sufficient to produce roughly ¾ of the amplitudes found in Fig. 5a. The first EOF (the diurnal cycle) explains 77.9% of the variance in JJA (compared to 69.2% for the full year), whereas EOF2 explains an additional 6.3% of the variance in JJA (compared to 8.7% for the full year). In short, convection was more strongly linked to the thermal forcing associated with the diurnal cycle in summer, which is not surprising. The maps of loadings for the first and second EOFs also were almost identical to those for the full year (Fig. 6), with the exception that for EOF2 the loadings were slightly more negative in the Piedmont region of North Carolina and Virginia during JJA. This would correspond to a more strongly delayed evening maximum in storms over the Piedmont during the summer months.

For brevity, we did not recreate all of the preceding figures for JJA, but the primary warm season features are summarized in Fig. 17. Because there are far more storms in the summer months, the amplitude of the residual was greater (again, by roughly a factor of 3; cf. Figs. 7 and 17). The primary streaks originating from the mountains and coast, e and g, remained and were almost identical to those in Fig. 7. Because the spring months were omitted, the signature of rapidly moving nocturnal episodes was diminished in the western part of the domain: streak a no longer appeared, and streak c was shorter and less distinct (although an additional streak, I, was identified; Fig. 17). The signal of eastward-moving storms developing over the Cumberland Plateau (streak f in Fig. 7) was no longer evident, although eastward-moving afternoon systems developing to the west of the terrain were more prominent in JJA (streak I in Fig. 17). Finally, the signal of nocturnal, offshore, eastward-moving storms became more distinct during JJA (streak H in Fig. 17); this may be associated with convection forced by land-breeze fronts over the ocean.

Although the details of the averaged streaks varied,

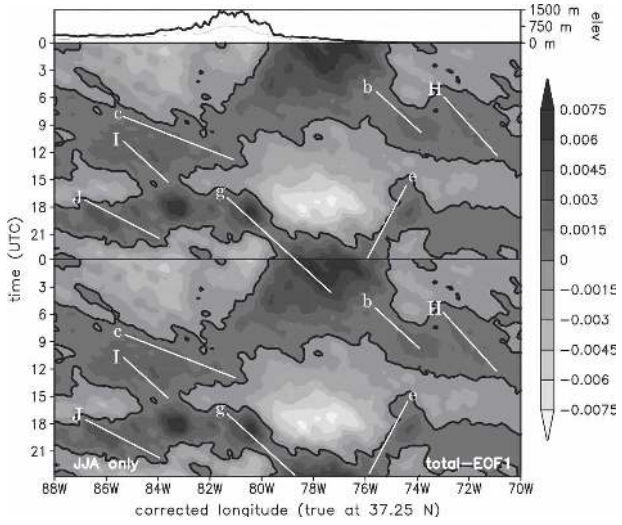

FIG. 17. Same as in Fig. 7 but for the months of Jun–Aug only. The objectively identified streaks (white line segments) are labeled for comparison with Fig. 7. Where there is close agreement, the lowercase letter from Fig. 7 is reused as a label. Other streaks that were not present in Fig. 7 are labeled with capital letters. Note that streaks a, d, and f from Fig. 7 do not appear.

the main difference between JJA and the full year (Figs. 7 and 17) was in the amplitude of the features. The patterns of storms were qualitatively very similar as a result of the fact that a large fraction of the storms in the dataset occurred during the summer months. Our full-year analyses have the benefit of completeness, because they include storms from throughout the year, and yet they do not appear to suffer much from noise associated with synoptic-scale forcing or bright bands in the cold season.

6. Summary

We investigated 9 yr of composited radar data in order to assess the frequency and character of organized convective systems in the east-central United States. The diurnal cycle's afternoon maximum is by far the most prominent signal in this part of the country. However, removing the principal component of variability associated with this afternoon maximum revealed the presence of convective systems via both temporally averaged fields and convective *episodes* that we objectively identified from Hovmöller diagrams.

Convective storms develop in the afternoon over the high terrain of the Appalachian Mountains, and most often move eastward into the Piedmont and the coastal plain. Some systems even survive past the coastline, and cross the warm waters of the Gulf Stream, which is just offshore in the Carolinas. These eastward-moving systems partly contribute to a delay in the daily maximum in thunderstorms across the corridor between the mountains and the coast.

Of the 2128 total episodes (236 yr^{-1}) that we identified, most (approximately 90%) were eastward movers. In addition to those developing over the mountains during the afternoon, convective systems frequently developed to the west of the mountains, or entered the study domain from the central United States. In particular, nocturnal MCSs from the Great Plains and the Ohio Valley frequently entered the domain at night. Such systems would then often arrive at the Appalachian cordillera around the time of the next day's diurnal maximum, providing a favorable situation for redevelopment of new storms over the high terrain. Roughly 10% of episodes starting west of the Blue Ridge were able to survive while crossing over to the eastern side; their chances were best when the crossing occurred around the time of the afternoon maximum in storms over the mountains.

The importance of vertical wind shear to organized convective storms is well established in the literature, and the present data support its importance in our study region. We found that the frequency of convective episodes peaked in the summer and dominated the annual statistics, a result that dovetails with the climatology of severe thunderstorm winds in the region. Although the southeastern United States is frequently perceived to lack baroclinicity and shear during the summer months, the summertime convective episodes occurred in above-average vertical wind shear. We restate that the diurnal mode is still the most important feature of regional convection. However, sufficient shear for the organization of convection appears to be present frequently in the region, such that convective episodes are common.

Several avenues for additional study may prove fruitful. The physical processes that govern mountain-crossing MCSs, and the possibly unique mechanisms for MCS generation by the Appalachian versus the Rocky Mountains, are of ongoing interest. As for applications, we are aware of one team that is investigating the severe weather climatology of Appalachian-crossing MCSs (Keighton et al. 2007). It would be of interest to know the likelihood that the other kinds of convective episodes (e.g., orogenic eastward movers, westward movers) are associated with severe weather and flooding; recent work by Garay et al. (2006) has shown that Hovmöller diagrams can be of great benefit in this regard. As well, regional forecasters have mentioned repeatedly observing convective systems that develop in Ohio or Pennsylvania and move southward across the study domain. Although we did not observe many such

systems when reviewing our radar animations, the climatology of such systems (which would have an artificial zonal speed in our skewed domain) may be worth exploring. Because most studies of organized convection have focused on the central United States to this point in time, the applicability of the reigning MCS conceptual models and forecast techniques in the eastern United States stands as an unanswered question.

Acknowledgments. The authors thank P. Banacos, M. Coniglio, S. Corfidi, R. Edwards, J. Guyer, G. Hartfield, K. Keeter, S. Keighton, L. Lee, Y.-L. Lin, A. Riordan, and R. Thompson for beneficial discussions/correspondence about this work, as well as the participants of the Warm Season Precipitation Workshop held in June 2006, and the Mid-Atlantic CSTAR Discussion Group. In addition, we particularly acknowledge R. Carbone, who provided many helpful suggestions and whose comments helped to improve this manuscript. The streak analysis was performed with the software and assistance of J. Tuttle, to whom we are greatly indebted. The first author receives support from the National Science Foundation under Grant ATM-0552154.

REFERENCES

Ahijevych, D. A., C. A. Davis, R. E. Carbone, and J. D. Tuttle, 2004: Initiation of precipitation episodes relative to elevated terrain. *J. Atmos. Sci.,* **61,** 2763–2769.

Augustine, J. A., and F. Caracena, 1994: Lower-tropospheric precursors to nocturnal MCS development over the central United States. *Wea. Forecasting,* **9,** 116–135.

Bonner, W. D., 1968: Climatology of the low level jet. *Mon. Wea. Rev.,* **96,** 833–850.

——, and J. Paegle, 1970: Diurnal variations in the boundary layer winds over the south central United States in summer. *Mon. Wea. Rev.,* **98,** 735–744.

Carbone, R. E., J. D. Tuttle, D. A. Ahijevych, and S. B. Trier, 2002: Inferences of predictability associated with warm season precipitation episodes. *J. Atmos. Sci.,* **59,** 2033–2056.

Coniglio, M. C., H. E. Brooks, S. J. Weiss, and S. F. Corfidi, 2007: Forecasting the maintenance of quasi-linear mesoscale convective systems. *Wea. Forecasting,* **22,** 556–570.

Cotton, W. R., R. L. George, P. J. Wetzel, and R. L. McAnelly, 1983: A long-lived mesoscale convective complex. Part I: The mountain-generated component. *Mon. Wea. Rev.,* **111,** 1893–1918.

Doswell, C. A., III, H. E. Brooks, and M. P. Kay, 2005: Climatological estimates of daily local nontomadic severe thunderstorm probability for the United States. *Wea. Forecasting,* **20,** 577–595.

Evans, J. S., and C. A. Doswell III, 2001: Examination of derecho environments using proximity soundings. *Wea. Forecasting,* **16,** 329–342.

Falconer, P. D., 1984: A radar-based climatology of thunderstorm days across New York state. *J. Climate Appl. Meteor.,* **23,** 1115–1120.

Farrell, R. J., and T. N. Carlson, 1989: Evidence for the role of the lid and underrunning in an outbreak of tornadic thunderstorms. *Mon. Wea. Rev.,* **117,** 857–871.

Frame, J., and P. Markowski, 2006: The interaction of simulated squall lines with idealized mountain ridges. *Mon. Wea. Rev.,* **134,** 1919–1941.

Fritsch, J. M., J. D. Murphy, and J. S. Kain, 1994: Warm-core vortex amplification over land. *J. Atmos. Sci.,* **51,** 1780–1807.

Gamache, J. F., and R. A. Houze Jr., 1982: Mesoscale air motions associated with a tropical squall line. *Mon. Wea. Rev.,* **110,** 118–135.

Garay, M. J., R. Fovell, and D. W. McCarthy, 2006: Filling the gap: Using severe storm climatologies to investigate the predictability and dynamics of precipitation episodes in the warm season. Preprints, *23rd Conf. on Severe Local Storms,* St. Louis, MO, Amer. Meteor. Soc., 1.6.

Grady, R. L., and J. Verlinde, 1997: Triple-Doppler analysis of a discretely propagating, long-lived, high plains squall line. *J. Atmos. Sci.,* **54,** 2729–2748.

Keighton, S., J. Jackson, J. Guyer, and J. Peters, 2007: A preliminary analysis of severe quasi-linear mesoscale convective systems crossing the Appalachians. Preprints, *22nd Conf. on Weather Analysis and Forecasting,* Park City, UT, Amer. Meteor. Soc., P2.18.

Koch, S. E., and C. E. Ray, 1997: Mesoanalysis of summertime convergence zones in central and eastern North Carolina. *Wea. Forecasting,* **12,** 56–77.

Lericos, T. P., H. E. Fuelberg, A. I. Watson, and R. L. Holle, 2002: Warm season lightning distributions over the Florida peninsula as related to synoptic patterns. *Wea. Forecasting,* **17,** 83–98.

Lorenz, E. N., 1956: Empirical orthogonal functions and statistical weather prediction. Sci. Rep. 1, Statistical Forecasting Project, Dept. of Meteorology, Massachusetts Institute of Technology, 49 pp. [NTIS AD 110268.]

Maddox, R. A., 1980: Mesoscale convective complexes. *Bull. Amer. Meteor. Soc.,* **61,** 1374–1387.

——, J. Zhang, J. J. Gourley, and K. W. Howard, 2002: Weather radar coverage over the contiguous United States. *Wea. Forecasting,* **17,** 927–934.

McNider, R. T., and R. A. Pielke, 1981: Diurnal boundary-layer development over sloping terrain. *J. Atmos. Sci.,* **38,** 2198–2212.

Parker, M. D., and R. H. Johnson, 2000: Organizational modes of midlatitude mesoscale convective systems. *Mon. Wea. Rev.,* **128,** 3413–3436.

——, and J. C. Knievel, 2005: Do meteorologists suppress thunderstorms? Radar-derived statistics and the behavior of moist convection. *Bull. Amer. Meteor. Soc.,* **86,** 341–358.

Raymond, D. J., and H. Jiang, 1990: A theory for long-lived mesoscale convective systems. *J. Atmos. Sci.,* **47,** 3067–3077.

Rickenbach, T. M., and S. A. Rutledge, 1998: Convection in TOGA COARE: Horizontal scale, morphology, and rainfall production. *J. Atmos. Sci.,* **55,** 2715–2729.

Rotunno, R., J. B. Klemp, and M. L. Weisman, 1988: A theory for strong, long-lived squall lines. *J. Atmos. Sci.,* **45,** 463–485.

Trier, S. B., and D. B. Parsons, 1993: Evolution of environmental conditions preceding the development of a nocturnal mesoscale convective complex. *Mon. Wea. Rev.,* **121,** 1078–1098.

Tripoli, G. J., and W. R. Cotton, 1989: Numerical study of an observed orogenic mesoscale convective system. Part I: Simulated genesis and comparison with observations. *Mon. Wea. Rev.,* **117,** 273–304.

Tucker, D. F., and N. A. Crook, 1999: The generation of a mesoscale convective system from mountain convection. *Mon. Wea. Rev.,* **127,** 1259–1273.

Tuttle, J. D., and R. E. Carbone, 2004: Coherent regeneration and the role of water vapor and shear in a long-lived convective episode. *Mon. Wea. Rev.,* **132,** 192–208.

——, and C. A. Davis, 2006: Corridors of warm season precipitation in the central United States. *Mon. Wea. Rev.,* **134,** 2297–2317.

Wallace, J. M., 1975: Diurnal variations in precipitation and thunderstorm frequency over the conterminous United States. *Mon. Wea. Rev.,* **103,** 406–419.

Wilks, D. S., 1995: *Statistical Methods in the Atmospheric Sciences.* Academic Press, 467 pp.

Wolyn, P. G., and T. B. McKee, 1994: The mountain-plains circulation east of a 2-km-high north–south barrier. *Mon. Wea. Rev.,* **122,** 1490–1508.

Zhang, D.-L., S. Zhang, and S. J. Weaver, 2006: Low-level jets over the mid-Atlantic states: Warm-season climatology and a case study. *J. Appl. Meteor. Climatol.,* **45,** 194–209.